AD-A098 336 MATERIALS RESEARCH LABS ASCOT VALE (AUSTRALIA) F/G 20/11
EXPERIMENTAL DETERMINATION OF STRESS INTENSITY IN A CRACKED CYL--ETC(U)
MAY 80 G CLARK
UNCLASSIFIED MRL-R-774 NL

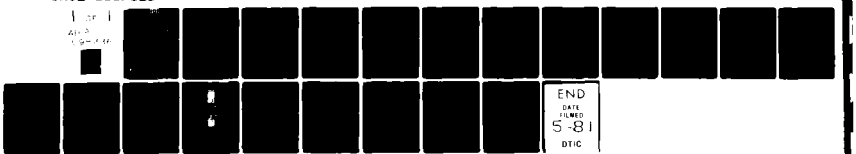

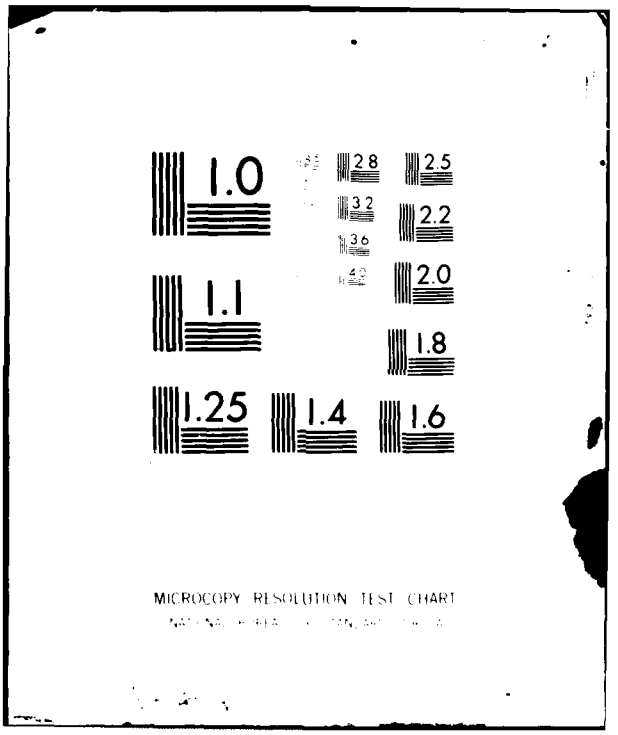
1.0
2.8
2.5
3.2
2.2
3.6
4.0
2.0
1.1
1.8
1.25
1.4
1.6
MICROCOPY RESOLUTION TEST CHART

MRL-R-774

LEVEL II

AR-002-157

12

DEPARTMENT OF DEFENCE

DEFENCE SCIENCE AND TECHNOLOGY ORGANISATION

MATERIALS RESEARCH LABORATORIES

MELBOURNE, VICTORIA

REPORT

MRL- R-774

EXPERIMENTAL DETERMINATION OF STRESS INTENSITY IN A CRACKED CYLINDRICAL SPECIMEN

Graham Clark

Approved for Public Release

MAY, 1980

DEPARTMENT OF DEFENCE

MATERIALS RESEARCH LABORATORIES

REPORT

(14) MRL-R-774

(6) EXPERIMENTAL DETERMINATION OF STRESS INTENSITY IN A CRACKED CYLINDRICAL SPECIMEN

(10) Graham Clark

(11) March 1980

(12) 27

ABSTRACT

The range of stress intensity at the tip of a fatigue crack is the major factor controlling the crack growth rate, and the relationship between these two parameters for any one material is easily established from crack growth rate measurements in a specimen geometry for which the stress intensity calibration is known. However, in a different specimen geometry made from the same material, different crack growth rates will be observed, and it is possible to use this relationship to determine the stress intensity calibration for the second geometry from a comparison of crack growth rates in the two specimens. This report describes such a stress intensity calibration procedure for a hollow cylindrical specimen containing a crack which grows radially from the bore under the influence of compressive loading across a diameter of the ring. The stress intensity determined experimentally is shown to be in close agreement with the results of a theoretical study.

Approved for Public Release

POSTAL ADDRESS: Chief Superintendent, Materials Research Laboratories
P.O. Box 50, Ascot Vale, Victoria 3032, Australia

DOCUMENT CONTROL DATA SHEET

Security classification of this page: UNCLASSIFIED

1. *DOCUMENT NUMBERS:*
   - a. *AR Number:* AR-002-157
   - b. *Series & Number:* REPORT MRL-R-774
   - c. *Report Number:* MRL-R-774

2. *SECURITY CLASSIFICATION:*
   - a. *Complete document:* UNCLASSIFIED
   - b. *Title in isolation:* UNCLASSIFIED
   - c. *Abstract in isolation:* UNCLASSIFIED

3. *TITLE:*

EXPERIMENTAL DETERMINATION OF STRESS INTENSITY IN A CRACKED CYLINDRICAL SPECIMEN

4. *PERSONAL AUTHOR(S):*

CLARK, Graham

5. *DOCUMENT DATE:* MAY, 1980

6. *TYPE OF REPORT & PERIOD COVERED:*

7. *CORPORATE AUTHOR(S):*

Materials Research Laboratories

8. *REFERENCE NUMBERS:*
   - a. *Task:* DST 77/069
   - b. *Sponsoring Agency:*

9. *COST CODE:* 514720

10. *IMPRINT (Publishing establishment)*

Materials Research Laboratories,
P.O. Box 50, Ascot Vale, Vic.3032

MAY, 1980

11. *COMPUTER PROGRAMME(S):*
(Title(s) and language(s)):

12. *RELEASE LIMITATIONS (of the document):*

Approved for Public Release

12-O. *OVERSEAS:* N.O. [ ] P.R. [1] A [ ] B [ ] C [ ] D [ ] E [ ]

13. *ANNOUNCEMENT LIMITATIONS (of the information on this page):*

No Limitation

14. *DESCRIPTORS:*

630 Stress concentration
Fatigue (materials)
Crack propagation
Test specimens

15. *COSATI CODES:* 1106 1113 2012

16. *ABSTRACT (if this is security classified, the announcement of this report will be similarly classified):*

The range of stress intensity at the tip of a fatigue crack is the major factor controlling the crack growth rate, and the relationship between these two parameters for any one material is easily established from crack growth rate measurements in a specimen geometry for which the stress intensity calibration is known. However, in a different specimen geometry made from the same material, different crack growth rates will be observed, and it is possible to use this relationship to determine the stress intensity calibration for the second geometry from a comparison of crack growth rates in the two specimens. This report describes such a stress intensity calibration procedure for a hollow cylindrical specimen containing a crack which grows radially from the bore under the influence of compressive loading across a diameter of the ring. The stress intensity determined experimentally is shown to be in close agreement with the results of a theoretical study.

CONTENTS

		Page No.
1.	INTRODUCTION	1
2.	EXPERIMENTAL STRESS INTENSITY CALIBRATION	3
3.	EXPERIMENTAL DETAILS	4
	3.1 Specimen Geometries	4
	3.2 Material	5
	3.3 Fatigue Loading	5
	3.4 Crack Length Monitoring	5
	3.5 Test Procedure	7
4.	CRACK GROWTH RATE RESULTS	7
5.	ANALYSIS OF RESULTS	8
	5.1 Determination of m	8
	5.2 Determination of Y_B	8
	5.3 Comparison of Experimental and Finite Element Calibration	9
6.	CONCLUSION	9
7.	ACKNOWLEDGEMENTS	9
8.	REFERENCES	10

* * *

EXPERIMENTAL DETERMINATION OF STRESS INTENSITY IN A CRACKED CYLINDRICAL SPECIMEN

1. INTRODUCTION

The recognition by Irwin [1] of the importance and usefulness of the stress intensity factor is one of the most significant events in the development of modern fracture mechanics. Using this parameter, it was possible (in principle at least) to describe in simple terms the elastic stress distribution at the tip of a sharp crack in a loaded body, and comparisons of crack growth behaviour in specimens with widely-differing geometries and loading systems became practicable. The development of a test procedure for the determination of the critical stress intensity at which unstable crack extension can occur (the material's fracture toughness K_{Ic}) led to the use of fracture toughness as a material selection parameter, and in many practical situations a minimum fracture toughness is now part of the materials specification for a component which is likely to be subjected to severe loading.

The majority of fracture mechanics procedures involve the use of a stress intensity (K) calibration for the geometry of interest. This usually takes the form

$$\frac{K\ B\ \sqrt{W}}{P} = Y \qquad (1)$$

where P is the applied load, and B and W are the specimen thickness and width respectively. The stress intensity calibration term Y varies as the crack length/specimen width ratio a/W increase, and is often presented as a polynomial in (a/W).

Stress intensity calibrations are available for many simple crack geometries and for a number of more complex practical situations in which the consequences of catastrophic failure are severe enough to justify a fracture mechanics analysis. Various techniques are used to obtain estimates

of Y; most of these involve extensive mathematical analysis (see for example Reference 2) and the choice of techniques is determined primarily by the geometry of the specimen and the loading conditions. It is unfortunate that, as the complexity of these factors increases, the difficulties encountered in applying mathematical techniques rapidly reduce the likelihood of obtaining a solution. In the last few years, however, the increasing availability of computing facilities has led to the widespread use of numerical techniques, such as finite element analysis, in which the specimen geometry is represented as a network (or mesh) of elements with specified elastic properties; the elastic behaviour of the whole mesh may then be determined by solving large numbers of simultaneous equations. Stress intensities may be obtained in various ways from these elastic stress and strain data. While the high cost of computing time is found to be offset in many situations by the near-certainty of being able to obtain a solution, there are many other cases in which these costs and the effort often required in mesh generation are prohibitive; this occurs most often when the computing facilities available are limited. The complexity of the numerical processing used in finite element and other numerical techniques can lead to a further problem when one crack situation is considered in isolation; the reliability of the result is not immediately apparent. While further confidence may be obtained by refining the mesh and running the program a second time (when little or no change in the result will usually indicate that the mesh is satisfactory), it is often impossible to find a means of confirming the numerical result.

Few experimental techniques have been used to determine stress intensities. This report describes the use of a method suggested by James and Anderson [3], based on establishing the relationship between fatigue crack growth rate and stress intensity for one material and then, by measuring crack growth rates in the geometry of interest, determining the stress intensity which produced these growth rates. The technique was originally suggested as a means of obtaining very rough estimates of stress intensity, and has found a few applications in failure analysis, where the observation of fatigue striations on a fracture surface can provide an estimate of crack growth rate immediately before failure of the component; experimental determination of the material's fatigue crack growth properties then allows an estimate to be made of the stress intensity which led to failure. However, it is clear that if suitably accurate measurements of fatigue crack growth rate can be made, and if the effects of material variation can be minimised, the technique is capable of providing stress intensity information from a very simple test program.

The experimental work described below involves growing fatigue cracks under conditions of limited crack tip plasticity; the specimens behave in an elastic manner, and hence only linear elastic fracture mechanics (in which crack tip plasticity is assumed to have only a small effect on both the crack tip stress field and the macroscopic behaviour of the specimen) is considered.

2. EXPERIMENTAL STRESS INTENSITY CALIBRATION

The application of repeated loading to a cracked specimen can result in the advance of the crack front by a fatigue mechanism under crack tip stress conditions considerably less severe than those required for instability in a rising-load test. Cyclic loading produces a range of stress intensity ΔK at the crack tip, and it is observed that the crack extension in each loading cycle (da/dN) is controlled primarily by ΔK, this relationship being well represented over a wide range of stress intensities by

$$\frac{da}{dN} = C(\Delta K)^m \tag{2}$$

where C and m are material constants requiring experimental determination.

The experimental technique used here involves the use of this fatigue crack growth rate relationship and the linear relationship between applied load and the stress intensity at the crack tip. Two specimen geometries are considered, and are assumed for convenience to have the same dimensions B and W. In practice, of course, this will not usually be the case, and simple corrections for any differences may be applied using equation [1].

Geometry A provides the reference data which are used to determine the relationship between crack growth rate and stress intensity for the material chosen, and has a known stress intensity calibration Y_A. Certain specimen geometries may provide sufficient variation in stress intensity and crack growth rate in one fatigue test conducted under a constant range of applied loading. In this case such loading conditions produce only a small variation in stress intensity, and the testing of two specimens (1 and 2) at different cyclic loads ΔP_1 and ΔP_2 is preferred. At any particular value of crack-length/specimen-width ratio (a/W), crack growth rates determined in the two specimens are related, from Equations (1) and (2), by

$$\frac{(da/dN)_1}{(da/dN)_2} = \left(\frac{\Delta K_1}{\Delta K_2}\right)^m = \left(\frac{\Delta P_1}{\Delta P_2}\right)^m \tag{3}$$

from which, knowing growth rates and loads in both specimens, a value of m may be determined. The approach used here is to compare crack growth rates at each of a number of values of a/W; if the test is carried out under loading which ensures that the stress intensity does not exceed the limits of validity of Equation (2), each comparison should yield the same value of the material constant m, and from the various estimates a mean value of suitable accuracy may be obtained. The test from which the stress intensity calibration for geometry B is determined need involve only one specimen of this geometry; a fatigue test is performed on this specimen, and crack growth rate measurements are made at various a/W values over the range of crack lengths for which a stress-intensity calibration is required.

At any particular value of a/W, a comparison may be made between crack growth rates in specimens of geometry B (with loading ΔP_3) and geometry A (with loading ΔP_1)

$$\frac{(da/dN)_B}{(da/dN)_A} = \left(\frac{\Delta K_B}{\Delta K_A}\right)^m = \left(\frac{\Delta P_3\ Y_B}{\Delta P_1\ Y_A}\right)^m \qquad (4)$$

and the value of the stress intensity calibration factor Y_B may then be determined from this expression for each crack-length/specimen-width ratio. These values represent the stress intensity calibration for geometry B.

3. EXPERIMENTAL DETAILS

3.1 Specimen Geometries

The possibility of failure of thick-walled pressure vessels arising from unstable growth of fatigue cracks had led to considerable interest in laboratory specimens consisting of rings cut from thick walled cylinders. Because applying loads to such specimens using internal pressure requires the manufacture of complex high pressure seals and the use of a high pressure cell, an alternative simpler system of growing fatigue cracks in cylindrical specimens has been proposed [4]. Compression of the ring across a diameter leads to high levels of tensile stress in the bore material nearest the loading point, and a crack which initiates in this region will grow radially through the wall towards the outside of the ring. Jones [4] considered rings with a radius ratio R (that is, the ratio of inner to outer radius) of 0.5 as shown in Figure 1(a), and produced a finite element stress intensity calibration for this configuration. The calibration, in the form of a curve fitted [5] to Jones' results, is shown in Figure 1(b), and has the interesting property of being almost flat over a wide range of crack lengths; in fact, the expression [5]

$$\frac{KB\sqrt{T}}{P} = 1.845 \qquad (5)$$

where B, T and P are defined in Figure 1(a), represents the calibration curve of Figure 1(b) to within ± 2.5% when $0.25 \leqslant a/T \leqslant 0.69$. The reason for interest in such a calibration curve is that if the specimen is subjected to a rising load fracture toughness test any crack extension will lead to little change in stress intensity, whereas in most fracture toughness specimen geometries any sub-critical crack growth may result in significant errors in the fracture toughness estimate obtained from the test.

The 76 mm gun tube forging currently manufactured in Australia is being used in an investigation of the effect of autofrettage residual stresses upon fatigue crack growth. Ring specimens with R = 0.555 are used in this work, and since Jones' results suggested that small departures from

an R value of 0.5 would prohibit the use of the calibration curve shown in Figure 1(b), an experimental stress-intensity calibration was performed for the R = 0.555 ring (geometry B), using Jones' specimen (R = 0.5) as a reference (i.e. as geometry A).

Specimens of geometries A and B were machined using the same wall thickness T (30 mm) in order to simplify data handling during and after the tests; a crack starter notch with a 90° included angle was machined at one point on each ring's inner surface, extending to a depth of 0.02 T. To remove any possible effects of differences in specimen thickness on either the crack length monitoring technique or the crack growth rate, all rings were machined to 25.4 mm thick.

3.2 Material

A major consideration in selecting a material for the specimens is the need to ensure that the fatigue properties of the materials used in the two geometries are as closely-matched as possible. In this particular case, this condition was met by machining the five specimens (two of geometry A, and three of B) from adjacent positions in the hollow gun tube forging, and ensuring that the test environment was identical for all tests. The material was a NiCrMoV gun steel with a 0.2% proof stress of approximately 1060 MPa although, as long as both types of specimen are made from materials with identical fatigue crack growth rate properties, the experimental calibration will be independent of these properties.

3.3 Fatigue Loading

Fatigue tests were carried out by compressing each ring specimen between two hardened steel platens in which shallow grooves conforming to the external radius of the ring had been machined in order to maintain specimen alignment with the axis of the testing frame. The load-distributing effect of these grooves would be expected to lead to some deviation from the ideal point-loading situation used for the reference calibration [4], but this effect was not considered likely to produce significant errors over the range of crack lengths used here. A 5 Hz sinusoidal fatigue load was applied using a 500 kN capacity MTS electrohydraulic testing machine, operating in load control mode; in all cases the ratio of minimum to maximum load in the cycle was 0.1, and loading was accurate to within 1%.

3.4 Crack Length Monitoring

Accurate fatigue crack length monitoring is clearly of crucial importance in cases such as this, where crack growth rates must be determined with high accuracy; in fact, inadequate crack length monitoring techniques, more than any other factor, have been responsible for a tendency to disregard the stress-intensity calibration procedure described here. For example, crack length monitoring by optical methods introduces a number of experimental errors, of which the most significant are the subjective nature of the technique and the unsuitability of a surface crack measurement technique for determining the mean of the various crack lengths throughout the specimen thickness. The latter problem prevents the measurement of a mean crack growth rate.

The potential drop (PD) technique, which usually involves passing a constant current through the test piece and monitoring the changing potential across the faces of the growing crack, does not suffer from such limitations and was used in these tests. A detailed description of the system used has been given elsewhere [6,7]; for this particular application, electrical connections for a constant DC current of 50 A (illustrated in Figure 2) were made by clamping contoured copper blocks to the external radius of the ring 90° from the notch, and the steel voltage probe wires were discharge-welded to the inner surface of the ring on each side of the notch at a distance T/2 from the diameter passing through the notch.

The PD calibrations relating the voltage across the crack (referred to that with no crack present, Vo) to the mean crack length for geometries A and B were obtained using analogue ring specimens of conducting paper, approximately 2 metres in diameter, to which electrical connections simulating those in the real specimens were made. With analogue specimens of this size, it is necessary to join several sheets of conducting paper with 'one-dimensional' electrical connections to prevent errors caused by overlapping two sheets of paper; these connections were made with a row of staples joining two separated sheets of paper. For calibration purposes, it was necessary to use much lower currents than those required in the real test, and control of the calibration procedure was improved by applying a constant voltage across the specimen, and monitoring the current flowing with a resistor-voltmeter system. The 'crack' was cut in the analogue specimen and changes in the current and the voltage across the probe wires were noted. The voltage across the crack was then corrected to model the real situation in which the current flowing through the specimen is constant, after which a polynomial of the form

$$a/T = \sum_{n=0}^{8} A_n \, (V/V_o)^{n/2} \qquad (6)$$

was fitted to the data, relating the crack-length/specimen-width ratio to the ratio of instantaneous to initial voltage. This particular form of polynominal differs from those used for many other fracture specimen geometries [6], in that a half-power series in (V/V_o) was found to provide a much better fit to the data than the usual power series (that is, Equation 6 with only even values of n).

During the fatigue test, the voltage across the crack faces is sampled at regular intervals, amplified, digitised and automatically presented as input to a desk calculator which determines the crack length from Equation (6) and estimates the crack growth rate. When the appropriate crack length is reached, or when various error conditions are detected, the calculator produces a signal which terminates the test. Further data handling is carried out [6] using a computer program which provides more accurate estimates of crack growth rates by fitting polynomials to sections of the crack-length/number-of-fatigue-cycles curve, and differentiating each polynomial.

3.5 Test Procedure

In this program five specimens were tested, although a stress intensity calibration for specimens of this type may be derived from only one test on geometry B, supported by two tests on geometry A. The test program details are shown in Table I.

T A B L E I

LOADS USED IN TEST PROGRAM

Specimen Geometry	Specimen Number	Max Load (kN)
Ring (radius ratio = 0.5)	A1	90
	A2	110
Ring (radius ratio = 0.555)	B1	90
	B2	90
	B3	70

The extra tests B2 and B3 made possible a determination of the reproducibility of crack growth rate determinations (in that specimens B1 and B2 should display the same crack growth rates), and additional determinations of m could be obtained, using the approach described in Section 2, from specimen pairs B1/B3 and B2/B3.

4. CRACK GROWTH RATE RESULTS

Figure 3 shows the variation of crack growth rate per load cycle with crack length for the five specimens tested. Several points are worth noting :

(a) The results of the duplicate tests B1 and B2 are in excellent agreement, with differences in da/dN of only some 2% in the central part of the curve. Whether this difference is associated with experimental conditions (such as errors in reading the small voltage across the crack or errors introduced by the crack length measurement system) or with differences in growth rate caused by material variations is not known.

(b) When a/T lies outside the range 0.25 to 0.75, da/dN falls away steeply, as would be expected from the form of the stress-intensity calibration in Figure 1(b) and the power-law relationship between da/dN and ΔK in Equation (2).

(c) There is a clear difference in the shape of the growth-rate/crack-length curves for the two specimen geometries, with the maximum growth-rate for geometries A and B being close to $\frac{a}{T} = 0.4$ and 0.5 respectively.

5. ANALYSIS OF RESULTS

5.1 Determination of m

Specimen pairs A2/A1, B2/B3 and B1/B3 were subjected to loads in the ratios 11/9, 9/7, 9/7 respectively, and the growth rate results from each pair were used in Equation (3) to provide estimates of the crack growth rate exponent m; values of m determined in this way at various crack lengths are shown in Figure 4. Over the crack length range $0.25 < a/T < 0.75$, in which crack growth rates do not change rapidly, m values from all three specimen pairs lie close to a single value. Outside the lower limit of this range errors in crack length estimates caused by crack front shape effects became significant [6], and errors introduced by the curve-fitting procedures used to estimate crack growth rates and to obtain a PD calibration curve are expected to increase when crack growth rates vary rapidly; the importance of these factors is reflected in the variations in m value estimates at crack lengths less than 0.25 T or greater than 0.75 T. The value of the material constant m to be used at later stages in the calibration procedure was estimated as 1.801 ± 0.087, this being the mean of 45 values obtained at intervals of T/30 within the range $0.25 < a/T < 0.75$.

5.2 Determination of Y_B

While a full statistical treatment of the results from such a small number of tests is not possible, an attempt was made to obtain an indication of the way in which errors in crack growth rate estimates affect the stress intensity calibration factor Y_B, by assuming that the differences in the results from duplicate tests B1 and B2 represent the experimental variations in the other tests. At various crack lengths, the greater of the growth rates for these two specimens was used with that for reference specimen A1 and a lower bound ($- 2\sigma$) estimate of m, to determine lower bound estimates of Y_B, from Equation (4). This procedure was then repeated, first using the lower of the B1 and B2 growth rates and the upper ($+ 2\sigma$) estimate of m, and then with mean values of the two growth rates and of m. In this way, a mean value of Y_B with an estimate of the limits within which the true value is expected to lie could be obtained at each crack length considered. These values (the calibration curve for geometry B) are shown in Figure 5, together with the corresponding values for geometry A, from Figure 1(b); as expected, a considerable difference exists between the stress intensity calibration for the two specimen geometries. Whilst too much significance should not be attached to the error bars in Figure 5, it is clear that the variation in the results obtained when tests are duplicated is small enough to support the wider use of this stress-intensity calibration procedure.

5.3 *Comparison of Experimental and Finite Element Calibration*

During the course of the test program described above, a finite element technique was used to perform a stress-intensity calibration for geometry B. The computer program used has been described by Jones and Callinan [8] and was used [9] for values of (a/T) ranging from 0.1 to 0.9. The results are shown in Figure 5, and the agreement between experimental technique and mathematical approximation is seen to be excellent.

In a comparison of the practical merits of the two techniques, both methods are seen to have advantages and disadvantages. For example, having determined the fatigue characteristics of the material experimentally, a stress intensity calibration for a different geometry can be performed by testing only one specimen of that geometry, but would require careful control of experimental conditions. The finite element technique, however, does not require any experimental work, but may be time consuming in that several meshes representing different crack lengths will usually be required for one calibration.

6. CONCLUSION

The use of a sensitive and accurate fatigue-crack growth rate measuring system has made possible the determination of the stress intensity calibration for a ring specimen geometry. The technique involved comparing crack growth rates in this geometry with those in a specimen for which the stress intensity calibration is known, and the results obtained are in excellent agreement with those produced by a finite element stress analysis.

7. ACKNOWLEDGEMENTS

The experimental work described in this report was carried out with the assistance of Mr. T.V. Rose, whose contribution is gratefully acknowledged.

8. REFERENCES

1. Irwin, G.R. (1957). Analysis of stresses and strains near the end of a crack traversing a plate. *J. Appl. Mech.*, 24, 361.

2. Tada, H., Paris, P.C. and Irwin, G.R. (1973). The stress analysis of cracks handbook. Del Research Corp., Hellertown, Pa.

3. James, L.A. and Anderson, W.E. (1969). A simple experimental procedure for stress intensity factor calibration. *Eng. Fract. Mech.*, 1, 565-568.

4. Jones, A.T. (1974). A radially cracked, cylindrical fracture toughness specimen. *Eng. Fract. Mech.*, 6, 435-446.

5 Grandt, A.F. (Jr.) (1977). Evaluation of a cracked ring specimen for fatigue testing under constant range in stress intensity factor. *Proc. Intl. Conf. Fracture Mechanics and Technology*, Hong Kong, March 21-25, 1977.

6. Clark, G. (1979). A high sensitivity potential drop technique for fatigue-crack growth measurements. *Report MRL-R-755*, Materials Research Laboratories, Melbourne, Australia.

7. Baxter, B.J. (1979). Data controller system for fatigue crack monitoring using a potential drop technique. *Technical Note MRL-TN-429*, Materials Research Laboratories, Melbourne, Australia.

8. Jones, R. and Callinan, R.J. (1976). A finite element method for calculating stress intensity factors in cracked sheet. *Structures Report 360*, Aeronautical Research Laboratories, Melbourne, Australia.

9. Clark, G. and Rose, T.V. (To be published).

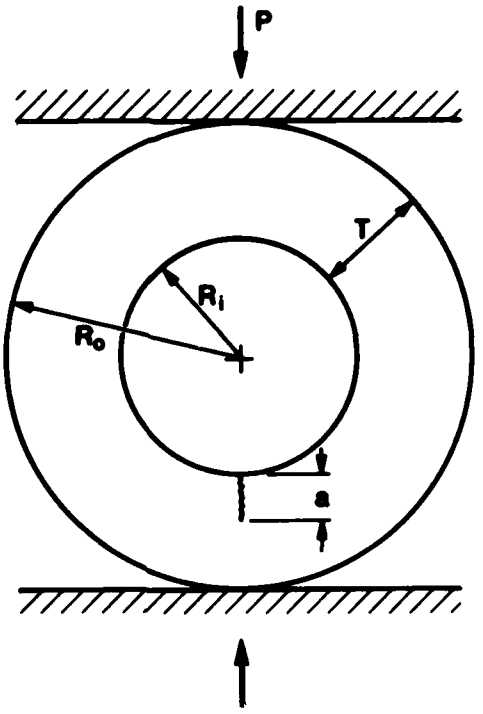

FIG. 1(a) - Ring specimen geometry (geometry A) considered by Jones [4]. The radius ratio $R = R_i/R_o = 0.5$.

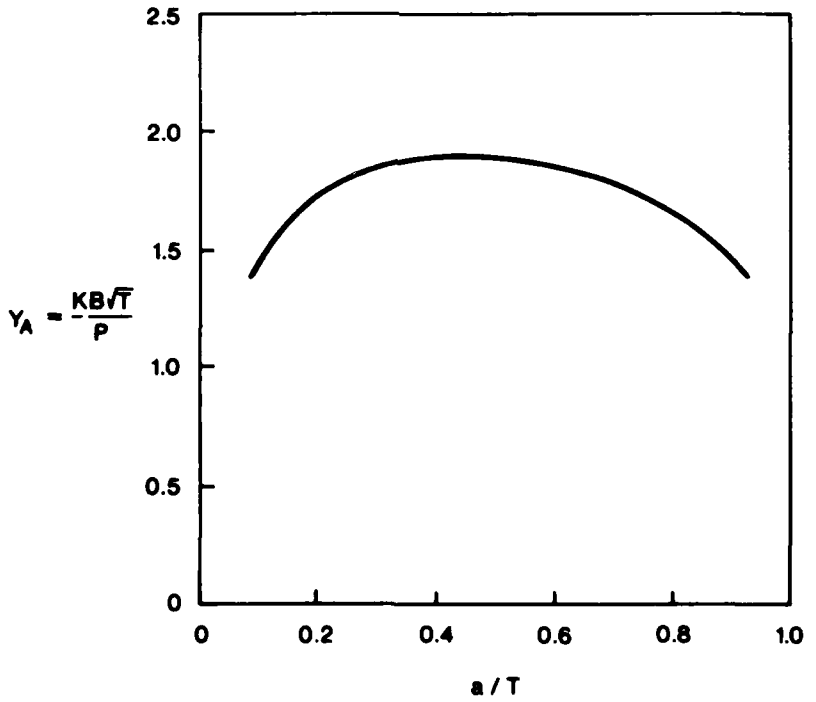

FIG. 1(b) - Stress intensity calibration curve for the geometry shown in Figure 1(a) (after Jones [4] and Grandt [5]). Between crack-length/specimen-width ratios 0.25 and 0.69, the dimensionless stress intensity calibration factor Y_A (= $KB\sqrt{T}/P$) varies by less than ± 2.5%.

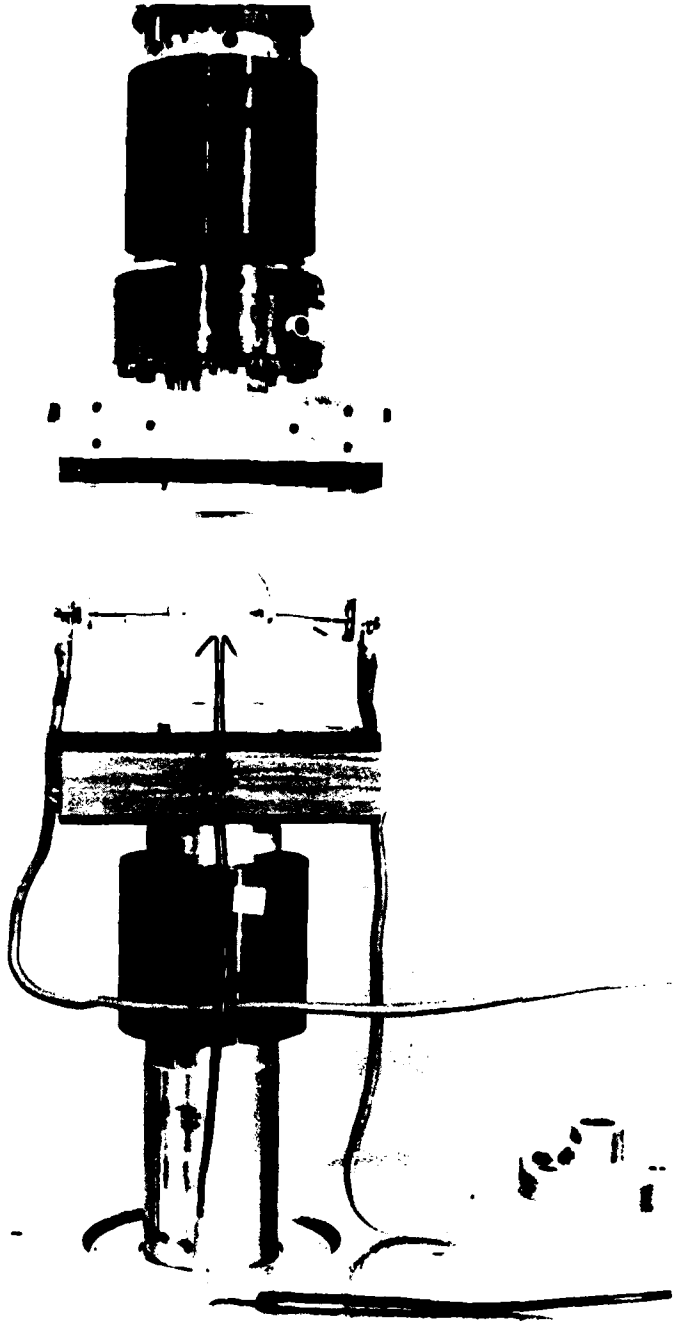

FIG. 2 - Specimen of geometry B under load in the testing frame, showing the copper blocks used to introduce the current for crack length monitoring, located 90° from the notch, and the voltage probe wires used to monitor the voltage across the crack faces.

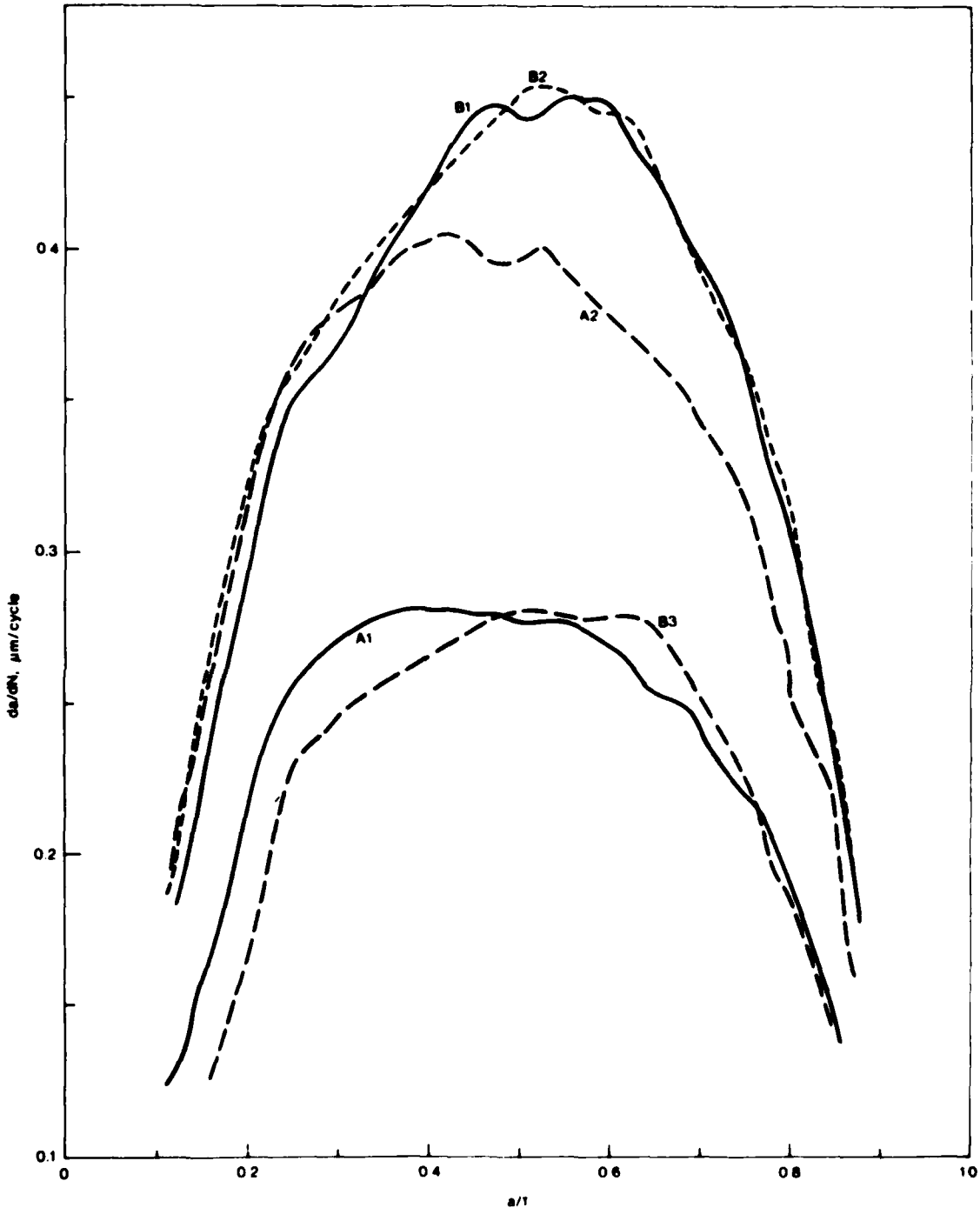

FIG. 3 - Crack growth rates, as a function of the crack-length/specimen-width ratio, for the five specimens tested.

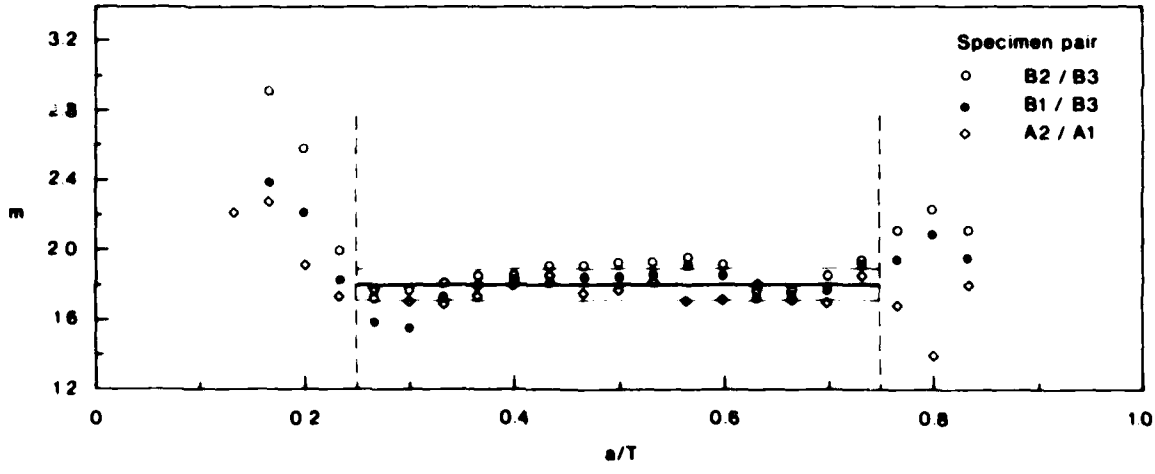

FIG. 4 - Values of the exponent m in Equation (2), determined by using the crack growth rate data from specimen pairs A2/A1, B2/B3 and B1/B3 in Equation (3). A mean value of the material constant m is shown; this was calculated from 45 estimates in the interval $0.25 < a/T < 0.75$. Outside this interval less consistent estimates are both expected and observed.

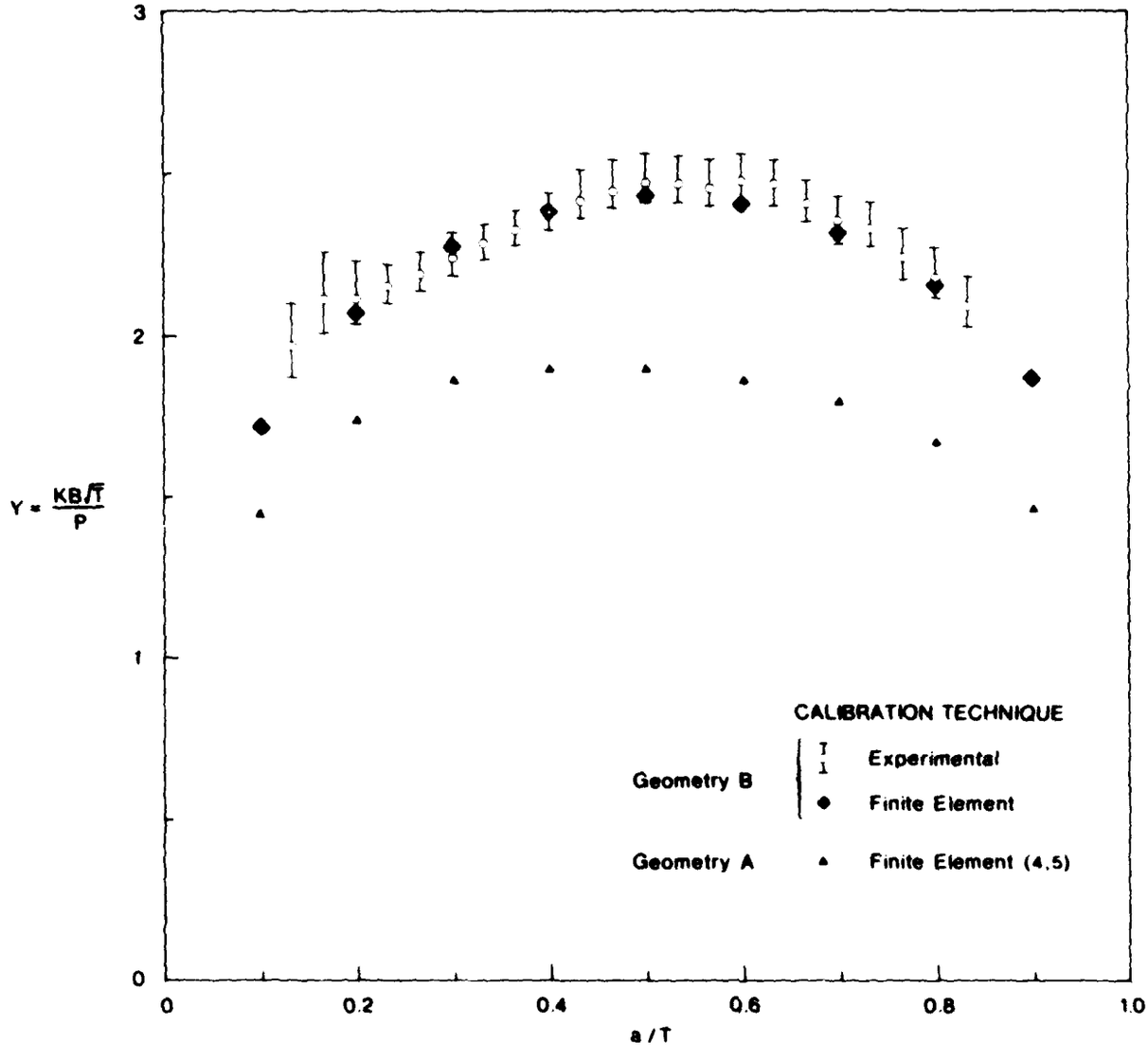

FIG. 5 - Stress intensity calibrations for geometry B (a ring with R = 0.555), obtained using both experimental and finite element techniques; agreement between the results for the two methods is excellent. The calibration for geometry A (a ring with R = 0.5) is also shown.

(MRL-R-774)

DISTRIBUTION LIST

MATERIALS RESEARCH LABORATORIES

Chief Superintendent
Superintendent, Metallurgy Division
Dr. M.E. de Morton
Dr. G. Clark
Library
Librarian, Materials Testing Laboratories, N.S.W. Branch
(Through Officer-in-Charge)

DEPARTMENT OF DEFENCE

Chief Defence Scientist
Deputy Chief Defence Scientist
Controller, Projects and Analytical Studies
Controller, Service Laboratories and Trials
Scientific Adviser - Army
Air Force Scientific Adviser
Navy Scientific Adviser
Chief Superintendent, Aeronautical Research Laboratories
Chief Superintendent, Weapons Systems Research Laboratory,
Defence Research Centre
Chief Superintendent, Electronics Research Laboratory,
Defence Research Centre
Chief Superintendent, Advanced Engineering Laboratory,
Defence Research Centre
Superintendent, Trials Resources Laboratory, Defence Research
Centre
Senior Librarian, Defence Research Centre
Librarian, R.A.N. Research Laboratory
Officer-in-Charge, Document Exchange Centre (16 copies)
Technical Reports Centre, Defence Central Library
Central Office, Directorate of Quality Assurance - Air Force
Deputy Director, Scientific and Technical Intelligence,
Joint Intelligence Organisation
Head, Engineering Development Establishment
Librarian, Bridges Library, Royal Military College

DEPARTMENT OF PRODUCTIVITY

NASA Canberra Office
Head of Staff, B.D.R.S.S. (Aust.)

DISTRIBUTION LIST

(Continued)

OTHER FEDERAL AND STATE DEPARTMENTS AND INSTRUMENTALITIES

The Chief Librarian, Central Library, C.S.I.R.O.
Australian Atomic Energy Commission Research Establishment

MISCELLANEOUS - OVERSEAS

Defence Scientific and Technical Representative, Australian High Commission, London, England
Assistant Director/Armour and Materials, Military Vehicles and Engineering Establishment
Reports Centre, Directorate of Materials Aviation, Orpington, Kent, England
Library - Exchange Desk, National Bureau of Standards, Washington, U.S.A.
U.S. Army Standardization Representative, C/o DGAD (NSO), Canberra, A.C.T.
The Director, Defence Scientific Information and Documentation Centre, Delhi, India
Colonel B.C. Joshi, Military, Naval and Air Adviser, High Commission of India, Red Hill, A.C.T.
Director, Defence Research Centre, Ministry of Defence, Kuala Lumpur, Malaysia
Exchange Section, British Library, Lending Division, Yorkshire, England
Periodicals Recording Section, Science Reference Library, British Library, Holborn Branch, London, England
Library, Chemical Abstracts Service, Columbus, Ohio, U.S.A.
INSPEC: Acquisition Section, Institution of Electrical Engineers, Hitchin, Herts, England
Overseas Reports Section, Defence Research Information Centre, Orpington, Kent, England
Engineering Societies Library, New York, U.S.A.

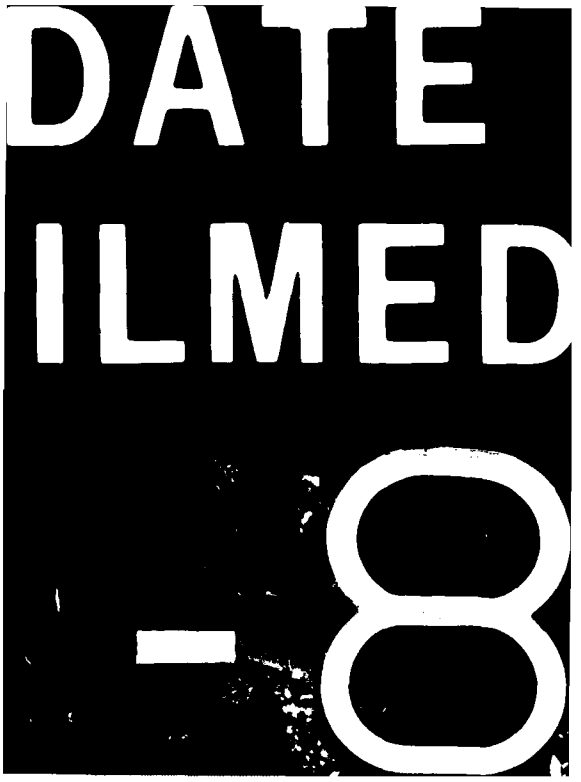
DATE
ILMED
-8